



BER and outage throughput analysis of DPIM/DHPIM coded QPSK-OFDM based outdoor optical wireless communications

Muhammad Naveed Shaikh¹, Salman Arain², Syed Rizwan Hassan², Sghaier Guizani³, Ateeq Ur Rehman^{4,*}, Habib Hamam^{5,6,7,8}

¹Department of Electrical and Computer Engineering, COMSATS University Islamabad, Islamabad, Pakistan

²School of Computing Sciences, Institute of Engineering and Fertilizer Research, Faisalabad, Pakistan

³Electrical Engineering Department, Alfaisal University, Riyadh, Saudi Arabia

⁴School of Computing, Gachon University, Seongnam, South Korea

⁵Faculty of Engineering, University de Moncton, Moncton, Canada

⁶Faculty of Graduate Studies and Research, Hodmas University College, Mogadishu, Somalia

⁷Sector of Research and Innovation, Bridges for Academic Excellence, Tunis, Tunisia

⁸School of Electrical Engineering, University of Johannesburg, Johannesburg, South Africa

ARTICLE INFO

Article history:

Received 30 March 2024

Received in revised form
27 July 2024

Accepted 30 August 2024

Keywords:

Atmospheric turbulence

Bit error rate

Modulation

Outage throughput

Optical wireless communication

ABSTRACT

With the growing demand for fast and reliable communication systems, particularly in outdoor environments, it is essential to investigate advanced encoding techniques. Digital Pulse Interval Modulation (DPIM) and Dual Header Pulse Interval Modulation (DHPIM) emerge as promising alternatives to traditional line coding methods, providing enhanced spectral efficiency and resistance to signal disruptions. This paper presents the performance of a Quadrature Phase-Shift Keying (QPSK) Orthogonal Frequency Division Multiplexing (OFDM)-based Optical Wireless Communication (OWC) system using these advanced encoding schemes. The analysis includes simulation results on QPSK-OFDM-based transmitter design, free space optical channel modeling based on Gaussian and log-normal distribution atmospheric turbulence, and recovery of input digital stream using the mentioned line coding techniques. The results demonstrate optimal bit error rate (BER) values for the QPSK-OFDM-based OWC system. The primary innovation of this research lies in the encoding schemes and their performance in outdoor optical wireless communication systems under turbulent conditions. Through extensive simulations and analysis, detailed insights into the bit error rate and outage throughput characteristics of DPIM/DHPIM coded QPSK-OFDM are provided, offering a unique perspective on the performance of these schemes in real-world scenarios. The findings not only highlight the optimal BER values achievable with the QPSK-OFDM-based OWC system but also offer insights into the system's ability to overcome transmission challenges under various atmospheric conditions.

© 2024 The Authors. Published by IASE. This is an open access article under the CC BY-NC-ND license (<http://creativecommons.org/licenses/by-nc-nd/4.0/>).

1. Introduction

The mushroom growth in the number of mobile devices has led to an increase in demand for capacity in cellular and wireless local area networks (Shafiq et al., 2022). The interconnection between billions of devices has triggered a quest for unexplored resources with regard to the radio frequency (RF)

spectrum. Optical wireless communication (OWC) is viewed as a potential substitute for conventional RF communication systems due to its key attributes, including low cost, high security, license-free nature, potentially large bandwidth, and is not affected by electromagnetic radiation (Giggenbach and Shrestha, 2022; Wang et al., 2017). The key challenge with regard to OWC is to deal with the channel impairments such as atmospheric turbulence (Padhy and Patnaik, 2021; Arshad et al., 2020; Escribano et al., 2020) and scintillation effects (Bosu and Prince, 2019; Shafi et al., 2024; Shaikh et al., 2012; Ali et al., 2023).

Atmospheric turbulences are characterized by different types of distribution functions (Kaimin et al., 2015; Aladeloba et al., 2012). The OWC link

affected by log-normal turbulence based on the weighted product of two correlated random variables is presented in Yang et al. (2017). Bit error rate performance of intensity modulation and direct detection (IM/DD)-orthogonal frequency division modulation (OFDM) based OWC system under Gaussian turbulence is analyzed in Tsonev et al. (2013). Recently, modulation schemes such as digital pulse interval modulation (DPIM) and dual header pulse interval modulation (DHPIM) modulation schemes have been recommended for OWC systems (Arain et al., 2017).

In this paper, DPIM and DHPIM are utilized as encoding techniques to implement the quadrature phase shift keying (QPSK)-(OFDM) encoded OWC system. The benefit of variable length of DPIM and DHPIM schemes is augmented by combining it with the robustness of interleaving characteristics of the OFDM symbol. The bit error rate (BER) performance of the proposed system is evaluated by considering atmospheric turbulence as a channel impairment. The Novelty of this study is the usage of the encoding schemes for QPSK-OFDM-based OWC systems under turbulent environments. To the best of the author's knowledge, the analysis of DPIM/DH-PIM encoded

QPSK-OFDM based FSO channel under a turbulent environment has been presented for the very first time in this paper.

2. System model

The transmitter and receiver design for the proposed DHPIM/DPIM encoded QPSK-OFDM-based OWC system is shown in Fig. 1. The transmitter encodes source bits by using either the DHPIM or the DPIM technique. The encoded bit stream is fed into a serial-to-parallel conversion block to be converted into the individual lower data rate parallel streams. These parallel data streams are modulated by a QPSK modulator and later mapped to OFDM frequency bins (Moussa et al., 2013). These frequency bins pass through an inverse fast Fourier transform (IFFT) block to perform frequency-to-time domain conversion. To avoid inter-symbol interference (ISI), a cyclic prefix is appended to the OFDM symbol. The time domain symbol is then transmitted through the OWC channel, where the signal suffers from atmospheric turbulence.

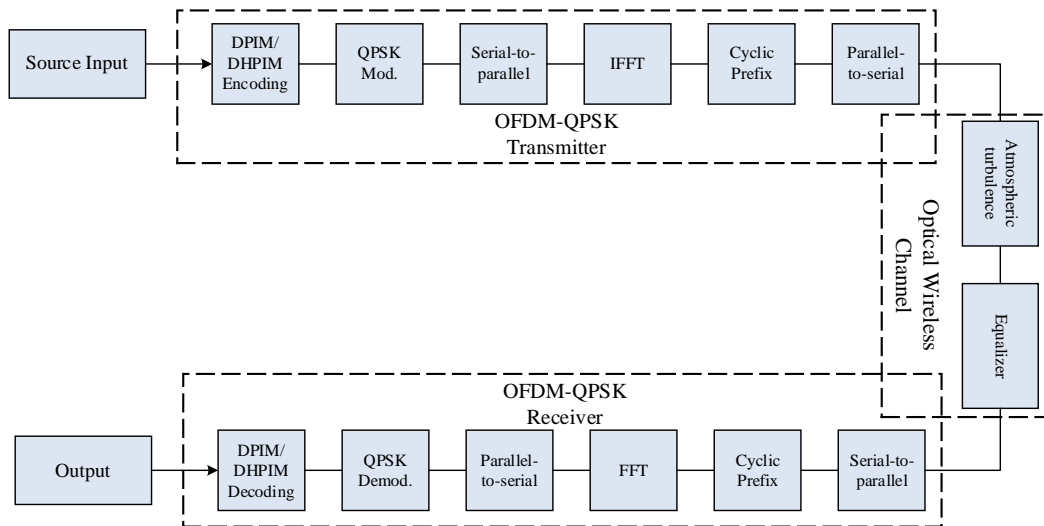


Fig. 1: Block diagram of DPIM/DHPIM QPSK OFDM transmitter

In Fig. 1, the receiver is implemented by passing the received signal through the blocks in reverse order to that of the transmitter, except for channel equalization, which is performed prior to demodulation.

3. Turbulence channel models

Atmospheric turbulence distribution is an important feature to characterize the OWC channel. This turbulence is mainly caused by temperature and refractive index variations observed in the path between the free space optics (FSO) transmitters and the receiver. The amplitude variations caused by atmospheric turbulence vary up to 10 dB, which leads to an increase in the probability of error (Wang et al., 2017). In this research work, Gaussian and log-

normal models (Ghassemlooy et al., 2019) are used as turbulence models. When initiating a new concept or setup, these models are widely accepted and used in the literature. Gaussian models are used for moderate turbulence conditions. On the other hand, log-normal models are preferable for stronger turbulence models. By implementing both those models in the proposed QPSK-OFDM-based optical wireless network, a broader range of atmospheric conditions are tested that may encountered by the outdoor optical wireless communication systems in the real world environment. The probability density function (PDF) of Gaussian atmospheric turbulence follows a normal distribution with $(\mu = 0, \sigma^2)$ is defined as:

$$f_{LN}(x; \mu, \sigma^2) = \frac{1}{\sigma\sqrt{2\pi}} e^{-\frac{(x-\mu)^2}{2\sigma^2}} \quad (1)$$

The distribution of log-normal atmospheric turbulence is given in [Epple \(2010\)](#) as:

$$f_{LN}(x; \mu, \sigma^2) = \frac{1}{x\sqrt{2\pi\sigma}} e^{-\frac{(\ln(x)-\mu)^2}{2\sigma^2}} \quad (2)$$

where, x denotes the coefficient of log-normal distribution with mean μ and standard deviation σ^2 . This σ is a function of the Rytov parameter σ_{eff} as reported in [Khandakar et al. \(2018\)](#):

$$\sigma = \exp\left(\frac{0.49\sigma_{eff}^2}{(1+1.11\sigma_{eff}^{12/3})^{7/6}} + \frac{0.51\sigma_{eff}^2}{(1+0.69\sigma_{eff}^{17/5})^{5/6}}\right) - 1 \quad (3)$$

The σ_{eff} determines the strength of the turbulence and defined by [Guo et al. \(2019\)](#) as:

$$\sigma_{eff} = 1.23C_n^2 k^{7/6} L^{11/6} \quad (4)$$

where, C_n is the scintillation index, $k = \frac{2\pi}{\lambda}$ is the wavenumber of the optical wavelength and L is propagate $\sigma_{eff} > 1$ in length.

The turbulence is considered as strong when $\sigma_{eff} > 1$. In case of $\sigma_{eff} < 1$, the turbulence effect is weak. Channel capacity or transmission capacity of DPIM/DPHIM encoded QPSK-OFDM OWC systems can be deduced using conventional Shannon's capacity relation ([Bi and Tang, 2019](#)) to provide transmission bandwidth for a specific set of OWC transceivers. Furthermore, outage capacity normalized with transmission capacity or loss in spectral efficiency can be deduced as in Eq. 5 using the approaches implemented in [Sharma et al. \(2023\)](#).

$$U = \log_2(1 + \gamma) B_{err} \quad (5)$$

In Eq. 5, U shows outage capacity in terms of bits per second per hertz, while γ and B_{err} are average signal-to-noise ratio and bit error rate, respectively.

4. Simulation results

In this section, we present the performance analysis of the proposed DHPIM/DPIM encoded QPSK-OFDM-based OWC system. All the simulations were performed by using MATLAB 2013 software. The transmitter, receiver, and system parameters are obtained from the specifications of practical systems ([Elsayed et al., 2022](#)), as shown in [Table 1](#). In this section, the BER of DPIM encoded OWC system is affected by Gaussian and log-normal turbulences, as shown in [Fig. 2a](#) and [Fig. 2b](#), respectively. The Gaussian and log-normal turbulences are characterized by their respective PDFs with variance denoted by σ^2 . The value of depends on the temperature and refractive index variations observed in the OWC.

In [Fig. 2a](#), BER versus Eb/No is plotted for the system affected by Gaussian turbulence at different values of σ^2 . It can be seen that as variance increases, the BER also increases. These results help quantify the impact of temperature and refractive index variations on the OWC. Moreover, to achieve a

particular threshold τ of BER, lower energy per bit is required for lower values of σ^2 . For example, at the BER threshold $\tau=10^{-2}$, the required energy per bit is 2.5dB for $\sigma^2=0.3$, but this required energy per bit increases up to 7 dB for $\sigma^2=0.9$. Similar results are shown for log-normal turbulence in [Fig. 2b](#). Furthermore, the comparison of Gaussian turbulence with log-normal turbulence reveals that to achieve $\tau=10^{-2}$, the energy per bit requirement in case of log-normal turbulence is higher than Gaussian turbulence.

In [Fig. 2a](#), BER versus Eb/No is plotted for the system affected by Gaussian turbulence at different values of σ^2 . It can be seen that as variance increases, the BER also increases. These results help quantify the impact of temperature and refractive index variations on the OWC. Moreover, in order to achieve a particular threshold " τ " of BER, lower energy per bit is required for lower values of σ^2 . For example, at the BER threshold $\tau=10^{-2}$, the required energy per bit is 2.5dB for $\sigma^2=0.3$, but this required energy per bit increases up to 7 dB for $\sigma^2=0.9$. Similar results are shown for log-normal turbulence in [Fig. 2b](#). Furthermore, the comparison of Gaussian turbulence with log-normal turbulence reveals that to achieve $\tau=10^{-2}$, the energy per bit requirement in the case of log-normal turbulence is higher than in Gaussian turbulence.

Table 1: Important simulation parameters

Parameter	Value
Wavelength	1550 nm
Data rate	1 Gbps
Laser power	10 dBm
RF frequency	20 GHz
Dark current	10 nA
Responsivity	1 A/W
Load resistance	1 K Ω

BER of DHPIM encoded OWC system affected by Gaussian and log-normal turbulence is shown in [Fig. 3a](#) and [Fig. 3b](#), respectively. The comparison of Gaussian and log-normal turbulences exhibit similar behavior as observed for the case of DPIM, i.e., the system affected by log-normal turbulence requires higher energy per bit to achieve the same τ for both encoding schemes. The DHPIM encoded QPSK-OFDM shows different BER performance for log-normal turbulence than DPIM encoding. For example, if the BER threshold $\tau=10^{-4}$ and $\sigma^2=0.3$, the required energy per bit is 7 dB in the case of DHPIM, but this required energy per bit is around 6.5 dB for DPIM.

The outage throughput in terms of bps/Hz is shown for DPIM-encoded OWC systems affected by Gaussian and log-normal turbulences in [Fig. 4a](#) and [Fig. 4b](#), respectively. For a fixed value of SNR, the loss in throughput is higher if variance is increased. This relative increase in outage throughput with increased variance is higher in log-normal turbulence. For instance, the value of the outage throughput is increased from 0.9 to 0.4 bps/Hz in Gaussian turbulence, while for a similar value of SNR, this increase is from 0.16 to 0.38 bps/Hz. The comparison of Gaussian and log-normal turbulences

exhibit similar effects on the outage throughput of DHPIM encoded QPSK-OFDM OWC systems behavior

as observed for the case of DPIM as shown in Fig. 5a and Fig. 5b, respectively.

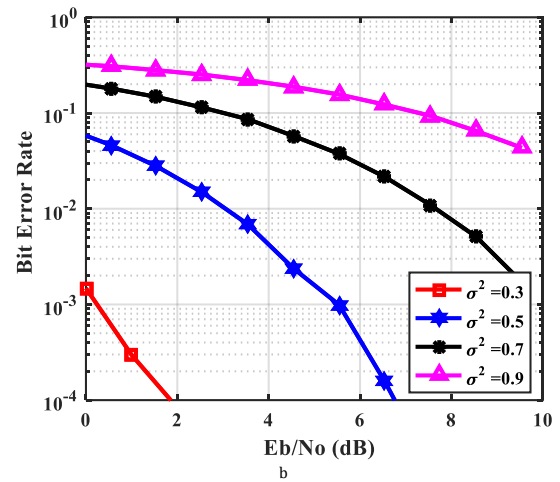
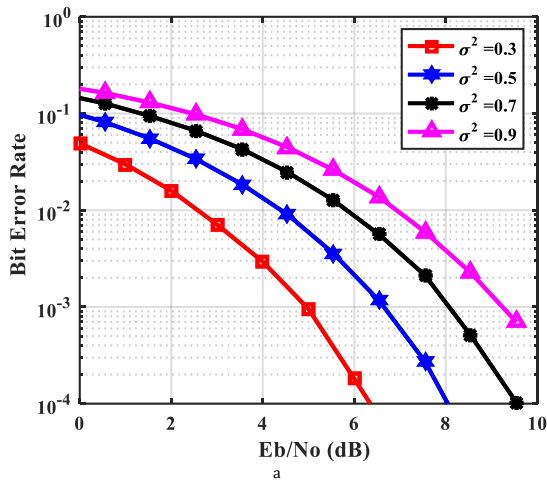


Fig. 2: BER performance of DPIM for the proposed encoded scheme over turbulence models (a) Gamma turbulence, (b) Log-normal turbulence

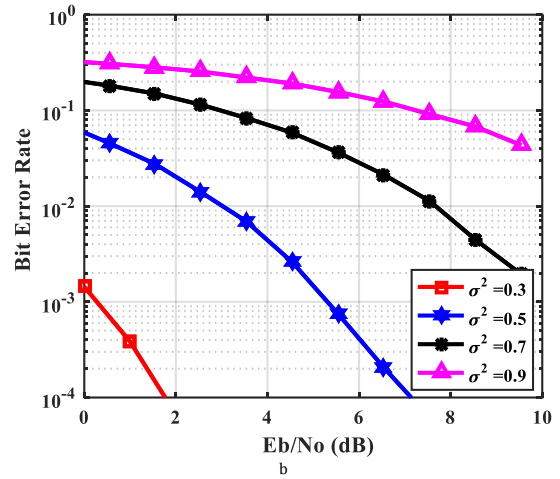
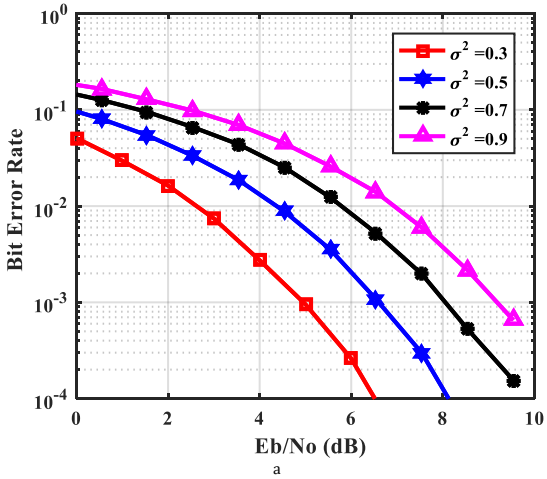


Fig. 3: BER performance of DHPIM for the proposed encoded scheme over turbulence models (a) Gamma turbulence, (b) Log-normal turbulence

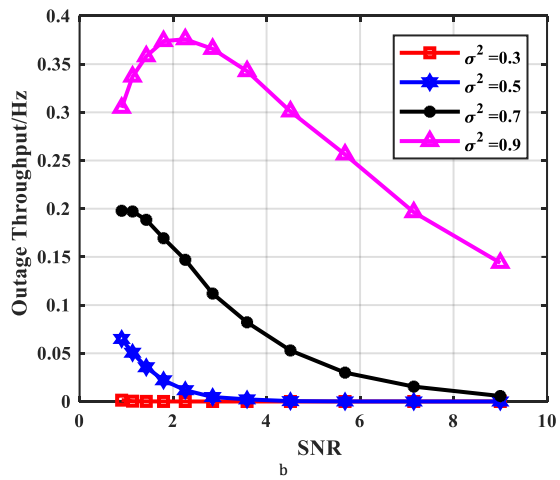
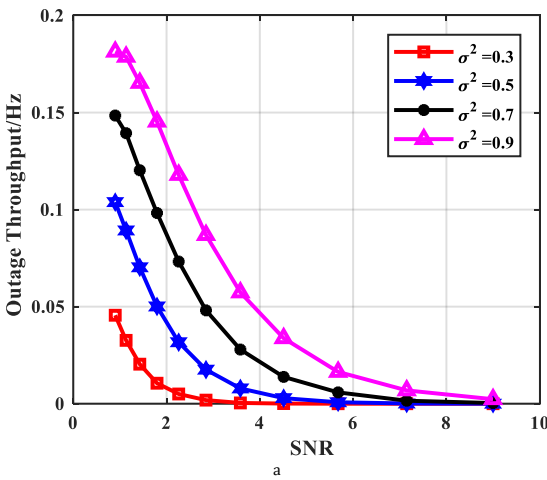


Fig. 4: Outage throughput performance of DPIM for the proposed encoded scheme over turbulence models (a) Gaussian turbulence, (b) Log-normal turbulence

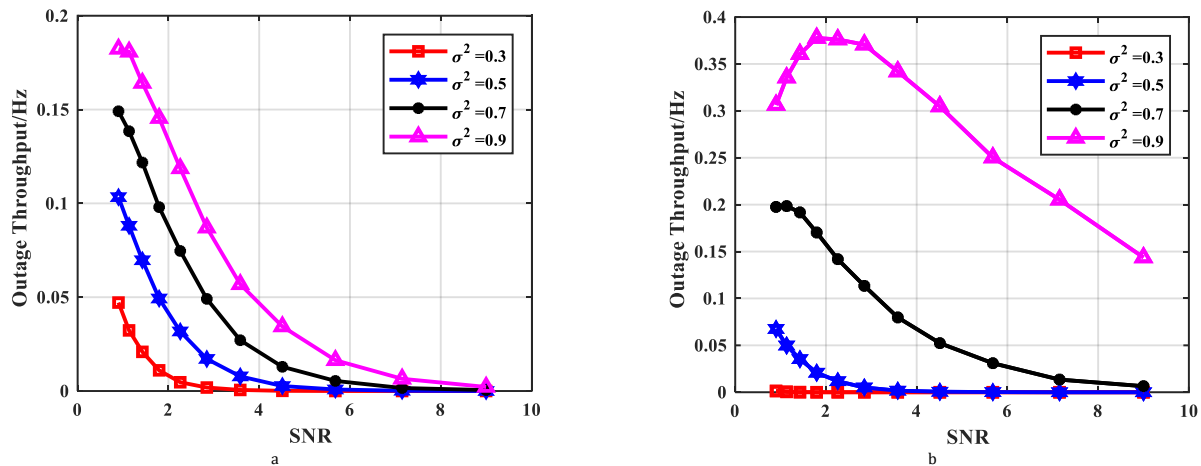


Fig. 5: Outage throughput performance of DHPIM for the proposed encoded scheme over turbulence models (a) Gaussian turbulence, (b) Log-normal turbulence

5. Limitations and future work

The proposed research has some limitations, particularly in addressing certain aspects of specific outdoor environments. Additionally, the findings may not apply broadly to other environmental scenarios. Further analysis should include additional performance parameters. Future research could involve incorporating more turbulence models and conducting experimental validations. Performance optimization and more robust analyses using different coding schemes could also be explored. Another area for future work is to integrate the proposed coding system with machine learning-based adaptive signal processing and free-space optical beamforming techniques.

6. Conclusions

This paper presents a BER analysis for DPIM/DHPIM encoded QPSK-OFDM in an Optical Wireless Communication (OWC) system. To account for the impact of atmospheric turbulence on the OWC channel, Gaussian and log-normal turbulence models are applied. The findings show that, for both DPIM and DHPIM encoding, QPSK-OFDM transmitters require higher energy per bit under log-normal turbulence than Gaussian turbulence to achieve the same BER. These results can guide the required energy per bit to meet specific BER targets. The study also examines the loss in spectral efficiency through outage throughput, measured as bits per second per unit hertz. It is shown that for both DHPIM and DPIM systems, outage throughput increases as the variance of Gaussian and log-normal turbulences rises, with this improvement corresponding to an increase in signal-to-noise ratio.

Compliance with ethical standards

Conflict of interest

The author(s) declared no potential conflicts of interest with respect to the research, authorship, and/or publication of this article.

References

- Aladeloba AO, Phillips AJ, and Woolfson MS (2012). Improved bit error rate evaluation for optically pre-amplified free-space optical communication systems in turbulent atmosphere. *IET Optoelectronics*, 6(1): 26-33. <https://doi.org/10.1049/iet-opt.2010.0100>
- Ali KS, Khan AA, Ur Rehman A, and Ouahada K (2023). Learned-SBL-GAMP based hybrid precoders/combiners in millimeter wave massive MIMO systems. *PLOS ONE*, 18(9): e0289868. <https://doi.org/10.1371/journal.pone.0289868> PMID:37682816 PMCID:PMC10490977
- Arain S, Shaikh MN, Waqas A, Ali Q, Chowdhry BS, and Themistos C (2017). Comparative study and packet error rate analysis of advance modulation schemes for optical wireless communication networks. *Wireless Personal Communications*, 95: 593-606. <https://doi.org/10.1007/s11277-016-3912-6>
- Arshad J, Rehman A, Rehman AU, Ullah R, and Hwang SO (2020). Spectral efficiency augmentation in uplink massive MIMO systems by increasing transmit power and uniform linear array gain. *Sensors*, 20(17): 4982. <https://doi.org/10.3390/s20174982> PMID:32887453 PMCID:PMC7506917
- Bi Y and Tang A (2019). On upper bounding Shannon capacity of graph through generalized conic programming. *Optimization Letters*, 13(6): 1313-1323. <https://doi.org/10.1007/s11590-019-01436-7>
- Bosu R and Prince S (2019). Mitigation of turbulence induced scintillation using concave mirror in reflection-assisted OOK free space optical links. *Optics Communications*, 432: 101-111. <https://doi.org/10.1016/j.optcom.2018.09.061>
- Elsayed EE, Alharbi AG, Singh M, and Grover A (2022). Investigations on wavelength-division multiplexed fibre/FSO PON system employing DPPM scheme. *Optical and Quantum Electronics*, 54: 358. <https://doi.org/10.1007/s11082-022-03717-5>
- Epple B (2010). Simplified channel model for simulation of free-space optical communications. *Journal of Optical Communications and Networking*, 2(5): 293-304. <https://doi.org/10.1364/JOCN.2.000293>
- Escribano FJ, Wagemakers A, Kaddoum G, and Evangelista JV (2020). A spatial time-frequency hopping index modulated scheme in turbulence-free optical wireless communication channels. *IEEE Transactions on Communications*, 68(7): 4437-4450. <https://doi.org/10.1109/TCOMM.2020.2987561>
- Ghassemlooy Z, Popoola W, and Rajbhandari S (2019). *Optical wireless communications: System and channel modelling with Matlab®*. 2nd Edition, CRC Press, Boca Raton, USA. <https://doi.org/10.1201/9781315151724>

- Giggenbach D and Shrestha A (2022). Atmospheric absorption and scattering impact on optical satellite-ground links. *International Journal of Satellite Communications and Networking*, 40(2): 157-176.
<https://doi.org/10.1002/sat.1426>
- Guo Y, Trichili A, Alkhazragi O, Ashry I, Ng TK, Alouini MS, and Ooi BS (2019). On the reciprocity of underwater turbulent channels. *IEEE Photonics Journal*, 11(2): 7901909.
<https://doi.org/10.1109/JPHOT.2019.2898094>
- Kaimin W, Bo L, Lijia Z, Qi Z, Qinghua T, and Xiangjun X (2015). Review of coded modulation free space optical communication system. *China Communications*, 12(11): 1-17.
<https://doi.org/10.1109/CC.2015.7365890>
- Khandakar A, Touati A, Touati F, Abdaoui A, and Bouallegue A (2018). Experimental setup to validate the effects of major environmental parameters on the performance of FSO communication link in Qatar. *Applied Sciences*, 8(12): 2599.
<https://doi.org/10.3390/app8122599>
- Moussa S, Razik AMA, Dahmane O, and Hamam H (2013). FPGA implementation platform for MIMO-OFDM based on UART. *Journal of Emerging Trends in Computing and Information Sciences*, 4(4): 367-371.
- Padhy JB and Patnaik B (2021). Link performance evaluation of terrestrial FSO model for predictive deployment in Bhubaneswar smart city under various weather conditions of tropical climate. *Optical and Quantum Electronics*, 53: 82.
<https://doi.org/10.1007/s11082-020-02702-0>
- Shafi F, Kumar A, and Nakkeeran R (2024). Performance analysis of free space optical networks under external limiting factors. *Results in Optics*, 14: 100615.
<https://doi.org/10.1016/j.rio.2024.100615>
- Shafiq M, Gu Z, Cheikhrouhou O, Alhakami W, and Hamam H (2022). The rise of "Internet of things": Review and open research issues related to detection and prevention of IoT-based security attacks. *Wireless Communications and Mobile Computing*, 2022: 8669348.
<https://doi.org/10.1155/2022/8669348>
- Shaikh MN, Waqas A, Chowdhry BS, and Umrani FA (2012). Performance and analysis of FSO link availability under different weather conditions in Pakistan. *New Horizons Journal of the Institution of Electrical and Electronics Engineers Pakistan*, 76: 3-8.
- Sharma R, Singh H, Goyal B, and Dogra A (2023). A single-channel 160 Gbps PDM-OFDM enabled integrated SMF-FSO transmission: Performance evaluation under external weather conditions. In the 4th International Conference on Electronics and Sustainable Communication Systems, IEEE, Coimbatore, India: 188-193.
<https://doi.org/10.1109/ICESC57686.2023.10193054>
- Tsonev D, Sinanovic S, and Haas H (2013). Complete modeling of nonlinear distortion in OFDM-based optical wireless communication. *Journal of Lightwave Technology*, 31(18): 3064-3076. <https://doi.org/10.1109/JLT.2013.2278675>
- Wang K, Gong C, Zou D, and Xu Z (2017). Turbulence channel modeling and non-parametric estimation for optical wireless scattering communication. *Journal of Lightwave Technology*, 35(13): 2746-2756.
<https://doi.org/10.1109/JLT.2017.2698440>
- Yang G, Li Z, Bi M, Zhou X, Zeng R, Wang T, and Li J (2017). Channel modeling and performance analysis of modulating retroreflector FSO systems under weak turbulence conditions. *IEEE Photonics Journal*, 9(2): 7902610.
<https://doi.org/10.1109/JPHOT.2017.2677501>